



## Investigation of Joints between AISI 1020 Carbon Steel and Monel400

### Produced by Friction Stir Welding

Mahmoud Abbas<sup>1</sup>, Mohamed M.Z. Ahmed<sup>2</sup>, Hamed.A.Abdel-Aleem<sup>3</sup>, Nada Azab<sup>4</sup>

<sup>1</sup> Suez University. Petroleum and Mining Engineering Faculty<sup>1</sup> Suez University. Petroleum and Mining Engineering Faculty, Department of Metallurgical and Materials Engineering, Assalam City, Suez, P.O. Box 43533, Egypt.

<sup>2</sup> mohamed.zaky@suezuniv.edu.eg

<sup>3</sup>(CMRDI) Central Metallurgical Research and Development Institute, Helwan, 11722 Egypt

<sup>4</sup> (SOPC) Suez Oil Processing Co. Suez, P.O. Box 100, Egypt



CrossMark

#### Abstract

Welding of both carbon steel (AISI 1020) and Monel 400 using friction stir welding is investigated in this article. The objective is to determine the effects of welding process variations in traverse and rotating speeds on joint quality. The traverse speed was adjustable among 50 and 100 mm/min, and the rotating speed was set between 200 and 400 rpm. It was found that 200 rpm rotational speed and 50 mm/min transversal speed produced best possible weld quality. And mainly 200 rpm rotational speed and 50 mm/min transversal speed produced the best possible weld quality. On the other hand, high transversal speeds of more than 200 mm/min produced flaws that resembled grooves. Three successive joints were accomplished (Monel400- Monel 400), (Monel 400- AISI carbon steel butt joint) and (Monel 400- AISI carbon steel lap joint). These welds' mechanical characteristics were thoroughly investigated at room-temperature. Tensile, impact, bending, and microhardness tests were held, the results of tensile test for three joints were 585MPa, 450MPa and 460MPa respectively, where for the hardness results were about 93 Kg/mm<sup>2</sup> and 81 Kg/mm<sup>2</sup> for Similar and Dissimilar joints. Metallurgical and mechanical tests showed that the joints had outstanding hardness, impact resistance. Scanning electron microscopy (SEM) and optical microscopy were used to analyze the alterations in the welds' microstructure.

**Keywords** (FSW) Friction stir welding. AISI1020 carbon steel· Mechanical characteristics. Monel400

#### 1. Introduction

Nickel-copper alloy known as Monel400 is remarkably corrosion-resistant in a variety of environments, including alkaline ones, seawater, and air conditions. This feature, together with the alloy's excellent ductility and ease of production, make it very appealing for a variety of industrial uses. Owing to its special qualities, Monel 400 is frequently utilized in reducing and oxidizing environments. Examples of these environments include chemical equipment, power plants, marine industry, and the manufacturing of a range of equipment, including heat exchangers, pumps, and valves [1].

AISI 1020 carbon steel has high toughness allows for easy machining, and its flexibility, along with relatively low strength, reduces the force required for forming processes. Additionally, its relatively low cost compared to other steel grades makes it an appealing choice for large-scale projects. With a tensile strength

ranging from 365 to 485 MPa, AISI 1020 demonstrates solid overall mechanical properties.

Dissimilar metal joints have widespread applications in the nuclear engineering, petrochemical, Automotive and other industries. These joints provide significant cost savings by reducing the need for new, costly materials in the production of numerous goods, while simultaneously meeting the unique needs of diverse service circumstances, such as heat and corrosion resistance. Sometimes, in order to satisfy design specifications, welding different metals together to create a single product is required. Another goal of combining different metals is to achieve specific specifications for particular applications. The process of joining different metals has grown more complex with recent improvements in the mechanical, physical, and metallurgical properties of these materials. Joints between AISI 1020 and Monel 400 are exposed to highly corrosive media, such as H<sub>2</sub>S, SO<sub>2</sub>, and SO<sub>3</sub>. Sadek and Abbas [2] studied dissimilar joints between

\*Corresponding author e-mail: [nada.m.azab@gmail.com](mailto:nada.m.azab@gmail.com)

Receive Date: 24 August 2024, Revise Date: 26 September 2024, Accept Date: 29 September 2024

DOI: 10.21608/ejchem.2024.314127.10254

©2024 National Information and Documentation Center (NIDOC)

carbon steel and Monel400, created using electrical welding, utilizing two filler materials.

Numerous studies have focused on the impact of FSW parameters on the properties of similar materials joined by friction stir welding. For instance, research has examined how welding speed affects the microstructural evolution and mechanical properties of friction stir welded Inconel 600 [3]. Another study explored the influence of rotational speed on the properties of Ti–6Al–4V alloys joined via FSW [4]. Additionally, the effect of alloying elements on the microstructure of dissimilar joints between Mg–Zn–Zr alloy (ZK60) and titanium produced by FSW was investigated. The joint exhibited an average tensile strength of 237 MPa, about 69% of that of ZK60, with failure occurring mainly in the stir zone of ZK60 and partially at the joint interface [5]. Microstructural evolution in the dissimilar FSW joint between 304 stainless steel and st37 steel has also been studied, where the process produced sound welds. In the stir zone of 304 stainless steel, refined grains were formed through dynamic recrystallization [6]. Furthermore, lap joining of dissimilar Ti and Al alloys by FSW demonstrated excellent surface appearance [7]. Finally, the effect of rotational speed on the microstructure and tensile strength of dissimilar friction stir welded aluminum alloy 6061 was also explored [8]. In this context, friction stir welding (FSW) has been developed as a novel way for joining divergent materials.

The current work aims to investigate the ability if these two metals to be welded and the fundamental properties of these dissimilar metal joints created through FSW [9, 10], investigating also the mechanical characteristics and the microstructural changes of the resulting weld. The ideal mechanical qualities for sound butt joints were achieved by adjusting the traverse and rotating speeds after varying between high range and find the best parameters for Friction Stir Welding these two metals.

Several researches have been conducted on the impact of FSW variables on the features of similar metals joined by the FSW method.

### Experimental Procedures

In this investigation, 3mm-thickness AISI 1020 Carbon Steel and Monel400 specimens were utilized as dissimilar materials.

Tables 1-4 provide the chemical compositions and mechanical characteristics of AISI1020 Carbon Steel and Monel400, respectively

Table (1) Chemical composition of AISI 1020 was indicated using XRF in EZZ El-Dekhela Co. as follow (wt%)

C	Mn	Si	P	S	Fe
0.193	0.652	0.22	0.006	0.002	Balance

Table (2) Chemical composition of Monel400 was indicated using XRF in SOPC as follow (wt%)

Ni	Cu	Fe	Mn	Mg	Co	Others
65.5	29.7	1.36	1.23	1.1	0.57	0.57

Table (3) AISI 1020 Mechanical properties

Tensile Yield	Strength, Ultimate	Tensile Strength, Ultimate	Strength, Break	Elongationat Break
310 MPa		450 MPa		26%

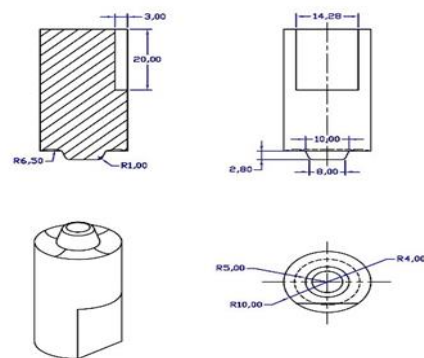
Table (4) Monel 400 Mechanical properties

Tensile Strength, Yield	Tensile Strength, Ultimate	Strength, Break	Elongationat Break
240 MPa	550 MPa		40%

According to previous researches on similar joints, the used tool in FSW was fabricated from tungsten carbide and a shoulder with a diameter of 20mm. As shown in Figures 1 and 2, the pin length for the butt joint was 2.8 mm, with the pin tapering from 10mm at the root to 8 mm at the tip.



Fig. (1) The used tool in FSW



Drawing No.	2.5	Title	FSW Tool
Scale	Scale to fit	Designer	Islam Badawy
Dimensions	mm	company	EgyStir

Fig. (2) showing the dimensions

Studying Radiographic inspection Radiography was used to inspect the produced joints (the source was Iridium-192 (Ir-192). for the joint showed sound welds among Monel400 and AISI 1020 Carbon Steel using friction stir welding. As shown in Fig (3)

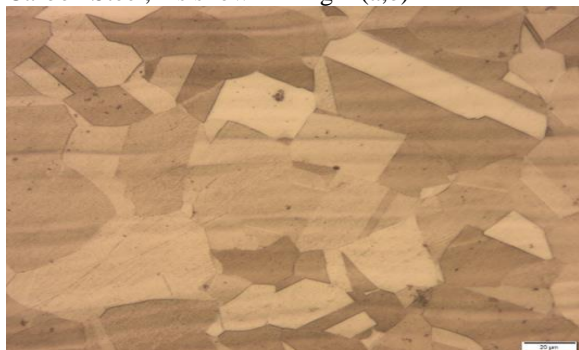


Fig. (3) Shows radiographic films for the dissimilar joint between Monel 400 and AISI1020 Carbon Steel using friction stir welding

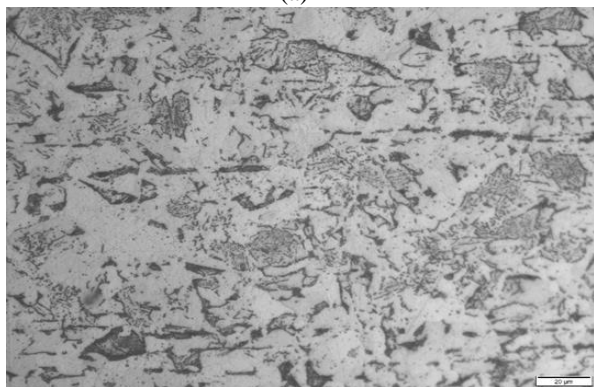
Figure 3 demonstrates that the AISI 1020 carbon steel and Monel 400 pair can be successfully joined using friction welding. No defects were found.

The test results indicate that the amount of flange proportionally with higher friction pressure, the optimal properties for the material welding were achieved with a rotational speed of 200rpm, friction load of 4000 kg and traverse speed of 50mm/min.

Equiaxed grains made up the elementary microstructure of Monel 400's microstructure, whereas ferrite and pearlite were present in AISI 1020 Carbon Steel, As shown in Fig 4 (a,b)



(a)



(b)

Fig. (4) Microstructure of: (a) Monel 400 (b) AISI 1020 Carbon Steel

The FSW process was made using rotating speeds of 200, 250, and 400 rpm, with traversal speeds of 50 and 100 mm/min according to the previous mentioned experiments in past researches [3-8].

The FSW process was made using rotating speeds of 200, 250, and 400 rpm, with traversal speeds of 50 and 100 mm/min according to the previous mentioned experiments in past researches [3-8].

The sheets were welded in a butt-joint arrangement, with a plunge depth of 3 mm. To make a microstructural examination, the samples were cut perpendicular to the FSW direction, then taken to polishing and etched according to standard procedures. sheets were welded with these variant parameters for several times and got many defects until the best joint parameters have been achieved, the specimens were etched by  $\text{HNO}_3:\text{FeCl}_3:\text{H}_2\text{O} = 30\text{ml}:500\text{g}:\text{per liter}$  for Monel400 [11]and Nital for Carbon steel in order to analyze the micro-structural evolutions. Optical microscopy was subsequently used to examine the sample. Additionally, hardness tests were conducted across the cross-section perpendicular to the welding line to study the hardness profile.

In addition, the tensile specimens were prepared with the grain direction-oriented opposite to that of the welding. The gauge area of the tensile samples included both the stir zone and the unaffected base metal. Then impact and bending tests were also conducted.

## Results and Discussion

### Metallographic Examination

Figure 5 shows the FSW joining zones of different materials, with AISI 1020 Carbon Steel depicted as the dark zone and Monel400 as the bright zone. The FSW was performed at traverse and rotational speeds of 50 mm/min and 200 rpm.

The stir zone (SZ) clearly shows a favorable mixture of the two alloys. Increasing the rotational speed or the ratio of rotational to traversal speed can gain greater deformation and an increase in the peak temperature of the thermal cycle. However, increasing the rotational speed, rises the strain rate also, reducing the time available for a fully recrystallized structure to form. On the other hand, at lower strain rates or rotational speeds, the higher peak temperature of the thermal cycle encourages the formation of recrystallized grains, which may then coarsen. [12]

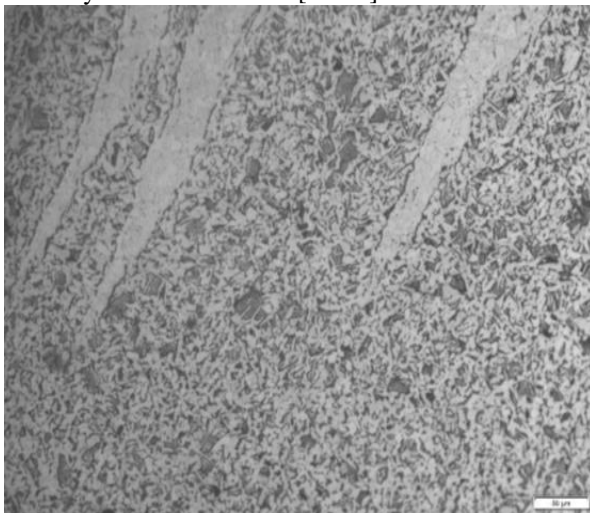




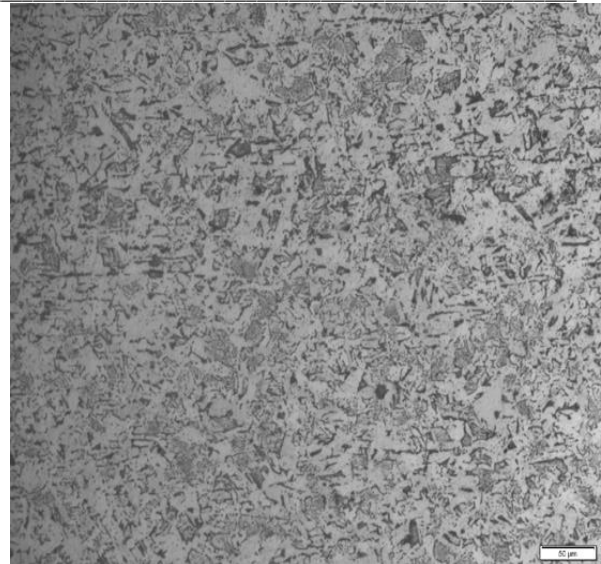
Fig. (5) FSW joining zones of Monel 400 with AISI 1020 Carbon Steel.

With reference to the FSW conducted at traverse and rotating speeds of 50 mm/min and 200 rpm, respectively. A complete blend of Monel400 and AISI 1020 Carbon Steel achieved at the ideal speeds of 50 mm/min and 200 rpm is shown in the SZ, as per Fig. 5.

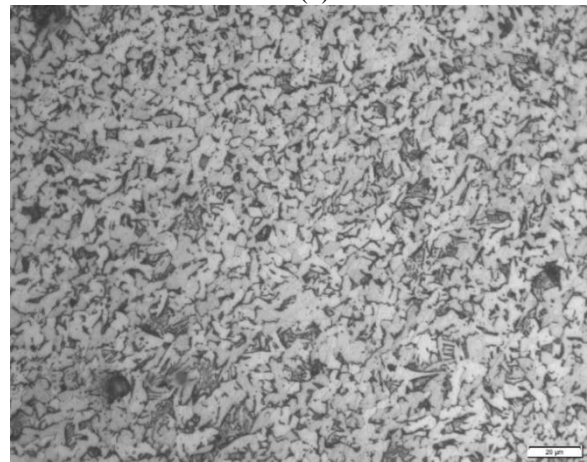
Figure 6a–c presents the microstructure of the three zones previously identified, corresponding to the FSW process conducted at traverse and rotational speeds of 50 mm/min and 200 rpm, respectively. As shown in Fig. 4, the stir zone (SZ) reveals a thorough mixing of Monel 400 and AISI 1020 Carbon Steel, achieved at the optimal speeds of 50 mm/min and 200 rpm. However, the heat-affected zone (HAZ) on the advancing side and the thermomechanically affected zone (TMAZ) on the retreating side were challenging to observe. The interface between the TMAZ and the stir zone (SZ) on the advancing side is more distinct than on the retreating side. This highlights the asymmetry of welds produced by FSW, as previously noted by other researchers. [13-15]



(a)



(b)



(c)

Fig.6: (a) The interface between TMAZ and SZ in the advancing side, (b) the region illustrating HAZ, TMAZ and SZ in retreating side (c) the SZ.

At a constant rotational speed, increasing the welding speed led to more pronounced grain refinement. This impact, in expansion to the preparing parameters, can be credited to the stacking fault energy (SFE) of Ni and Cu [16]. Generally, materials with low SFE cannot undergo dislocation rearrangement through mechanisms of dynamic recovery. In other words, materials with low SFE promptly form powerfully recrystallized grains. As a result, stable grain nuclei can create amid thermomechanical forms like FSW when the SFE is low [17]. Figure 7 is showing the microstructure of the stir zone (SZ) in the sample subjected to FSW at traverse and rotational speeds of 50 mm/min and 200 rpm, respectively. Also figure 8 is showing SEM analysis for the stir zone.

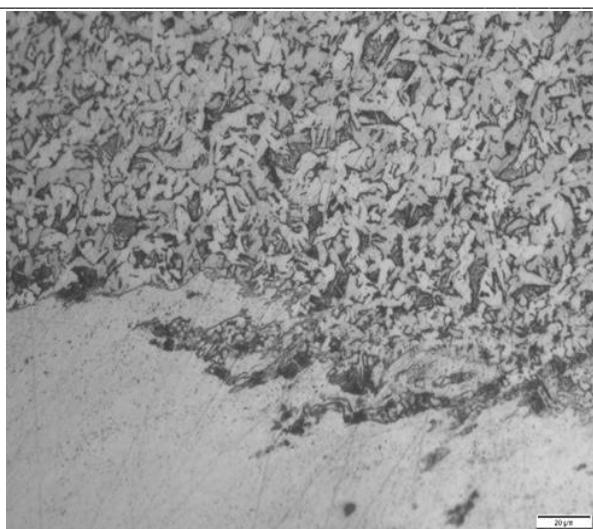


Fig. (7) Cross-section showing the interference between Monel 400 and AISI 1020 carbon steel. Obviously, there is a desirable mix of two alloys in the SZ.

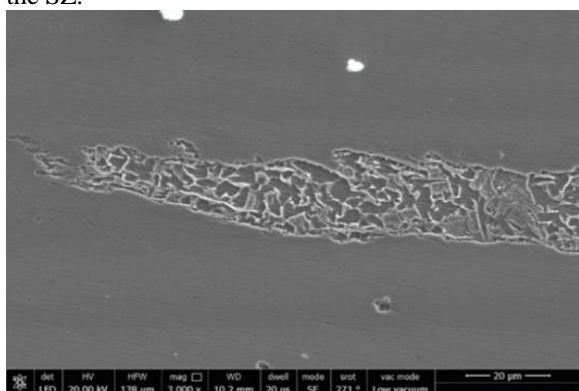
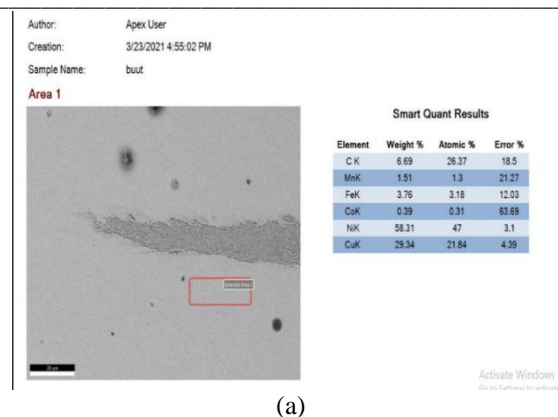


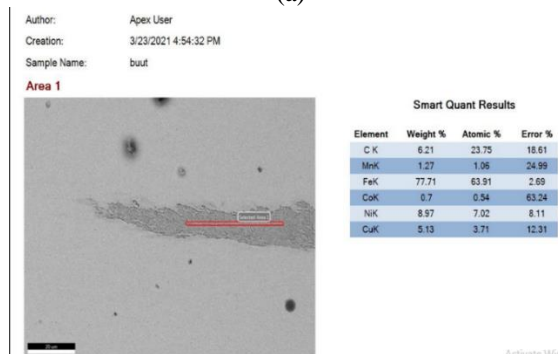
Fig. (8) is for SEM image that is taken from SZ

To investigate element diffusion across the interface and analyze the formation of intermetallic compounds, an area scan test was performed along the red line, as shown in Figure 9(a,b). The area scan results revealed the distribution profiles of Fe, Cu, Mn, C, Si, and Ni across the interface in the stir zone (SZ). The weight percentages of Cr, Mn, and Ni in Monel 400 were higher compared to AISI 1020 carbon steel, while the weight percentage of Fe was lower. Due to the high temperature and plastic deformation in the SZ, Cu, and Ni solutes diffused toward the AISI 1020 side, while Fe diffused toward the Monel 400 side.

As a result, moving from the AISI 1020 side to the Monel 400 side, the concentrations of Cu, and Ni increased, while the Fe concentration decreased.



(a)



(b)

Fig. (9) EDX results: (a) Area analysis for Carbon steel inside Monel400-AISI 1020 joint , (b) Area analysis for Monel 400 steel inside Monel400-AISI 1020 joint

**Mechanical Properties**

**Tensile Strength**

The tensile specimens fractured in the region corresponding to the AISI 1020 carbon steel, which has a lower ultimate tensile strength (UTS) than both Monel 400 and the weld. The UTS observed in this region was similar to that of the AISI 1020 carbon steel base metal, indicating that the fracture occurred in the weakest part of the weld. According to API 1104 [18] and ASME IX [19], Table 4.1 presents the approximate UTS values for the two base metals, a Monel400-Monel400 joint, and a dissimilar weld joint between AISI 1020 carbon steel and Monel 400.



Monel400                      AISI 1020

Fig. (10) tensile specimen for Monel 400 AISI 1020 Carbon Steel



Table (5) Results of tensile test:

Specimens	Monel base metal	AISI 1020 carbon steel	Monel – C.Steel
Tensile strength (UTS) MPa	585	450	460

### Hardness Measurements

Hardness test according to ASTM E384 shown in table (6-7).

Table (6): Results of the hardness test

Monel400 (Kg/mm2)	AISI 1020 Carbon Steel (Kg/mm2)	AISI 1020 Carbon Steel – Monel400 (Kg/mm2)
94.8	90.23	81.94
90.89	90.53	80.88
93.22	90.00	81.02

Table (7): The Average results for hardness

onel-Monel(butt)	92.97 Kg/mm2
Monel- AISI 1020(butt)	81.28 Kg/mm2

It was pointed out that the average hardness in the stir zone (SZ) was remarkably higher than that of both alloys. This was followed by a decrease in hardness in the heat-affected zones (HAZs) on both the retreating and advancing sides.

The first zone encountered when moving from AISI 1020 Carbon Steel to Monel 400 was the AISI 1020 Carbon base metal (BM). This zone exhibited the lowest hardness in the macro-hardness profile, consistent with the ferrite and pearlite microstructure typical of carbon steels. The measured hardness values aligned well with the findings of previous researchers [20].

### Impact Test

The absorbed energy at the weld metal center line is represented by the mid-thickness of the specimen and the intersection of the fusion line on both sides. The relatively high toughness observed in FSW could be attributed to the fine grain structures in the weld metal, HAZ, and TMAZ. The impact values for the joint produced by FSW are presented in Table 8.

Table (8) absorbed energy value in the FSW joint

Test temp C	Impact value (j)
Room temp.	21.8

### Bending Test

Figure 11 shows that neither of the two welds exhibited any cracks or defects, which may indicate the formation of sound welds. According to ASME B31.3 [21] and API 1104 [22], the bend test is considered satisfactory as long as no cracks or other imperfections larger than 1/8 inch (3 mm) are present, this emphasize that this kind of FSW dissimilar joints exhibited superior mechanical properties, which is highly desirable from a joint design perspective.



Fig. (11) Bending specimens

### Conclusion

1. When the FSW process was used with the chosen parameters, excellent welds free of cavities and fractures between AISI 1020 Carbon Steel and Monel 400 were created.
2. Using EDX and XRD for microstructural examination of the FSW weld metals, no intermetallic compounds were found.
3. The FSW welds exhibited a basin-shaped cross-section with alternating layers of carbon steel and Monel 400. Four distinct microstructures were identified in the welds. In addition to the two base metals, the HAZ of carbon steel displayed both partially and fully grain-refined regions. The SZ of carbon steel underwent recrystallization due to hot deformation during FSW, resulting in transformed grains with two microstructures (ferrite and pearlite) after cooling.
4. The impact value of the joints was acceptable for dissimilar joints, the Stir Zone hardness of the Friction Stir Welding weld rose, and the tensile test revealed a ductile fracture. The bending test revealed no flaws or cracks in the FSW-produced joints.
5. Because of the significant grain refinement inside the weld and HAZ, the FSW joint's ultimate tensile strength was reasonably high and met API 1104 and ASME IX requirements.

### 4 References

1. Ventrella V.A, Berretta JR, de Rossi W. "Microstructure development in Nd: YAG laser welding of AISI 304 and Inconel 600", Doi: <https://doi.org/10.1080/09507110903568877>, Physics Procedia 12:347-354 (2011)
2. Alber A.S, Mahmoud A. "Investigation of Dissimilar Joints Between Low Carbon Steel and Monel 400" trans JWRL, Vol. 29,(2000), No.1
3. Song KH, Fujii H, Nakata K "Effect of welding speed on microstructural and mechanical properties of friction stir welded Inconel 600". Doi:

- <https://doi.org/10.1016/j.matdes.2009.05.033>, Materials & Design, 30:3972–3978(2009)
4. Zhou L, Liu HJ, Liu QW. “Microstructural characteristics and mechanical properties of friction stir welded joints of Ti–6Al–4 V titanium alloy”. Doi: <https://doi.org/10.1016/j.matdes.2009.12.014>, Materials & Design 31:2631–2636(2010)
  5. Aonuma M, Nakata K. “Dissimilar metal joining of ZK60 magnesium alloy and titanium by friction stir welding”. Doi: <https://doi.org/10.1016/j.mseb.2011.12.031> Materials Science and Engineering, B 177:543–548(2012)
  6. Jafarzadegan M, Feng AH, Abdollah-zadeh A, Saeid T, Shen J, Assadi H “Microstructural characterization in dissimilar friction stir welding between 304 stainless steel and st37 steel”. Doi: <https://doi.org/10.1016/j.matchar.2012.09.004>, Materials Characterization, 74:28–41 (2012)
  7. Yu-hua C, Quan NI, Li-ming KE, “Interface characteristic of friction stir welding lap joints of Ti/Al dissimilar alloys”. Doi: [https://doi.org/10.1016/S1003-6326\(11\)61174-6](https://doi.org/10.1016/S1003-6326(11)61174-6) Transactions of Nonferrous Metals Society of China, 22:299–304(2012)
  8. Dinaharan I, Kalaiselvan K, V SJ, Raja P “Effect of material location and tool rotational speed on microstructure and tensile strength of dissimilar friction stir welded aluminum alloys”. Doi: <https://doi.org/10.1016/j.acme.2012.08.002>, Archives of Civil and Mechanical Engineering, 12:446–454. (2012)
  9. Satyanarayana V.V., Reddy G.M., Mohandas T “Dissimilar metal friction welding of austenitic-ferritic stainless steels” Journal of Materials Processing Technology, Volume 160, Issue 2, Pages 128-137, 20 March (2005)
  10. Moreira PMGP., Santos T., Tavares SMO., Richter-Trummer V., Vilaça P., de Castro PMS. “Mechanical and metallurgical characterization of friction stir welding joints of AA6061-T6 with AA6082-T6”, Materials & Design, Volume 30, Issue 1, Pages 180-187, January (2009)
  11. Deepakkumar H.P, Sadaiah M. “Some Investigations on Surface Texturing on Monel 400 Using Photochemical Machining” DOI:10.1115/MSEC2015-9294 Conference: ASME 2015 International Manufacturing Science and Engineering Conference At: North Carolina University, Charlotte, USA Volume: Paper No. MSEC2015-9294, pp. V001T02A045; 6 pages. June (2015)
  12. Mishra R.S., Ma Z.Y. ” Friction stir welding and processing” Materials Science and Engineering: R: Reports Volume 50, Issues 1–2, Pages 1-78, 31 August (2005)
  13. Sato Y.S., Nelson T.W., Sterling C.J., Steel R.J., Pettersson C.O. “Microstructure and mechanical properties of friction stir welded SAF 2507 super duplex stainless steel” Materials Science and Engineering: A Volume 397, Issues 1–2, Pages 376-384, 25 April (2005)
  14. Abdollah-zadeh A., Saeid T. “Weldability and mechanical properties of dissimilar aluminum-copper lap joints made by friction stir welding” Doi: <https://doi.org/10.1016/j.jallcom.2009.10.127>, Journal of Alloys and Compounds Volume 490, Issues 1–2, Pages 652-655, 4 February (2010)
  15. Schneider J.A., Nunes A.C. “Characterization of plastic flow and resulting micro textures in a friction stir weld” Metallurgical and Materials Transactions B 35(4):777-783, August (2004)
  16. JAMES M.H. “Interfaces in Materials: Atomic Structure, Thermodynamics and Kinetics of Solid-Vapor, Solid-Liquid and Solid-Solid Interfaces” Wiley-Inter science ISBN: 978-0-471-13830-3, 544 pages, February (1997)
  17. Humphreys F.J., Hetherly M. “Recrystallization and related annealing phenomena” Elsevier, Amsterdam, Boston. (2004)
  18. The American Petroleum Institute (API STANDARD 1104), “Welding of pipeline and related facilities”. 20th Edition (2005) 1- 82.
  19. The American Society of Mechanical Engineers (ASME SECTION IX), “Qualification standard for welding and brazing procedures, welders, brazers, and welding and brazing operators”. (2009) 1-138.
  20. Cavaliere P., Squillace A., Panella F. “Effect of welding parameters on mechanical and microstructural properties of AA6082 joints produced by friction stir welding” Journal of Materials Processing Technology, Volume 200, Issues 1–3, Pages 364-372, 8 May (2008)
  21. ASME B31.3,” ASME Code for Pressure Piping, Process Piping. (2015), 1-135.
  22. The American Petroleum Institute (API STANDARD 1104), “Welding of pipeline and related facilities”. 20th Edition (2005) 1- 82